

Video Article

Use of Decellularized Mammalian Lung Tissues to Study Cell: Matrix Interactions

Christina N. Blaul^{1,2}, Jenna Balestrini^{3,4}, Hongyi Pan⁵, Julia Winkler⁵, Erica L. Herzog⁵, Huanxing Sun⁵

¹NSF Funded Biomedical MD-PhD REU in affiliation with Yale School of Medicine, Yale Pathology Department, Section of Pulmonary, Critical Care, and Sleep Medicine, Yale University School of Medicine

²School of Natural Sciences: Molecular and Cellular Biology, University of California, Merced

³Department of Anesthesiology, Yale School of Medicine

⁴Cell Bioprocessing, Draper

⁵Department of Internal Medicine, Section of Pulmonary, Critical Care, and Sleep Medicine, Yale School of Medicine

Correspondence to: Erica L. Herzog at erica.herzog@yale.edu, Huanxing Sun at huanxing.sun@yale.edu

URL: <https://www.jove.com/video/55167>

DOI: [doi:10.3791/55167](https://doi.org/10.3791/55167)

Keywords: extracellular matrix, decellularization, bioengineering, interstitial lung disease, pulmonary fibrosis, cellular phenotype, translational medicine, lung scaffolds

Date Published: 9/8/2018

Citation: Blaul, C.N., Balestrini, J., Pan, H., Winkler, J., Herzog, E.L., Sun, H. Use of Decellularized Mammalian Lung Tissues to Study Cell: Matrix Interactions. *J. Vis. Exp.* (), e55167, doi:10.3791/55167 (2018).

Abstract

Adult lung homeostasis is maintained by a balance of cellular processes within the tissue microenvironment. The extracellular matrix (ECM) serves a critical role in this context both by supporting organ structure and by integrating signals from a variety of stromal and recruited cell populations via interactions involving both biochemical and biophysical cues. Disruption of this interplay engenders an injury response that if excessive, prolonged, or unrepaired can lead to permanent tissue disruption and organ failure. Efficient repair of tissue injury is thought to represent a continuum of responses involving structural cells, resident and recruited inflammatory cells, and activated tissue fibroblasts that require an intact ECM possessing the proper composition and physical characteristics. The use of ECM scaffolds prepared from decellularized organs have recently gained widespread implementation in the study of lung biology. Application of this method to the study of lung remodeling and repair demonstrates that decellularized lung scaffolds contain biophysical and biochemical cues that direct fate specification in a multitude of cells. Because studies of human lung tissue will be limited by the scarcity of starting material as well as the cost and sophistication of bioreactor-based recellularization strategies, it is necessary to scale down the decellularization and engraftment procedures from the entire lung to small segments of fresh lung tissue. The below protocol presents a decellularization system amenable for using fresh mammalian tissue obtained from both mice and humans and presents a representative recellularization and analytical algorithm that can be modified for tissues and cells from many sources.

Video Link

The video component of this article can be found at <https://www.jove.com/video/55167/>

Introduction

Adult lung homeostasis is maintained by a balance of cellular processes within the tissue microenvironment^{1,2,3}. The extracellular matrix (ECM) serves a critical role in this context both by supporting organ structure and by integrating signals from a variety of stromal and recruited cell populations via interactions involving biochemical and biophysical cues^{4,5,6}. Disruption of this interplay by endogenous or exogenous stimuli causes an injury response that, if prolonged, excessive, or unrepaired, can lead to permanent tissue disruption and organ failure^{7,8,9}. These processes are thought to represent a continuum of responses resulting from incompletely understood interactions between structural cells, resident and recruited inflammatory cells, and activated tissue fibroblasts¹⁰ that require an intact ECM¹¹. However, due to the complex and numerous aspects of these interactions, *ex vivo* simulation of cell: matrix interactions is difficult to achieve in available experimental systems. Therefore, the generation of models that faithfully recapitulate the microenvironments of both the healthy and diseased lung remains a critical unmet need.

Methods adapted from commonly used bioengineering techniques have emerged as novel platforms to study the interactions between cells and their local environment. The use of scaffolds prepared from decellularized organs, which was first described more than three decades ago, has recently gained widespread implementation in this regard¹². We refined this technique as the structural basis for the *ex vivo* generation of organotypic, functional lungs that are suitable for implantation and gas exchange *in vivo*⁴. Recent application of this method to the study of lung remodeling and repair demonstrates that the composition and physical structure of decellularized lung scaffolds obtained from normal and diseased lungs influence the fate specification of a multitude of cells^{4,13,14}. Acellular matrices have been particularly useful in the study of human lung fibrosis, a difficult to treat condition characterized by the accumulation of excessive and compositionally aberrant ECM^{5,15,16,17}. Because studies of human lung tissue will be limited by the scarcity of starting material as well as the cost and sophistication of bioreactor-based recellularization strategies, it is necessary to scale down the decellularization and engraftment procedures from the entire lung to small segments

of fresh lung tissue. Thus, the objective of our study was to develop a simulation of the fibrotic lung microenvironment that can be used for *ex vivo* studies of cell: matrix interactions in a variety of contexts. The below protocol presents a decellularization system amenable for the use of freshly obtained mammalian tissue obtained from both mice and humans and presents a representative recellularization and a representative analytical algorithm that can be modified for tissues and cells from many sources.

Protocol

All of the procedures including animal use have been approved by Institutional Animal Care & Use Committee (IACUC) of Yale University. The use of human tissues and cells has been approved by Yale's Human Investigation Committee (HIC).

1. Mouse Lung Slice Decellularization Protocol

1. Preparation of slices

1. Treat the mouse (C57/BL6, 6 to 8 weeks old, both male and female mice were used) with a lethal i.p (intraperitoneal) injection of Urethane or other anesthetic (2 g/kg)¹⁸. When mouse is deeply sedated and no longer responsive to paw pinch, perform median thoracotomy followed by bronchoalveolar lavage and right ventricular perfusion with phosphate buffer saline (PBS)^{19,20}.
NOTE: The Urethane solution includes heparin at 100 units/mL for anticoagulation²¹.
2. Remove the lungs *en bloc* and then separate into single lobes¹⁹. Place each lobe into a 60-mm sterile Petri dish.
3. Transfer the lung-containing 60-mm Petri dish to a 100-mm Petri dish. Put these two Petri dishes in the liquid nitrogen container together in order to float the Petri dishes on the surface of the liquid nitrogen and the tissue will be snap frozen to allow precise slicing. Using sterile technique, slice each lobe into 1 mm slices with a multi-knife.
NOTE: Do not let the tissue contact the liquid nitrogen directly. It is ok if some liquid nitrogen flowing in the 100-mm Petri dish. However, avoid the liquid nitrogen flowing in the 60-mm Petri dish.
4. Rinse slices extensively with PBS containing sodium nitroprusside (SNP) at 1 µg/mL for 1 h.
NOTE: Prepare 1 µg/mL SNP before use, no more than 24 h, sterilize via a 0.45 µm filter and protect from light.

2. Decellularization

1. Transfer the slices to a 15-mL tube that contains 5 mL of decellularization (decell) solution. Roll tube at 37 °C overnight with a shaker at 8 rpm.
NOTE: Wear a mask when preparing and using decell solution. Open CHAPS ((3-[(3-CholamLdopropyl)dimethylammonio]-1-propanesulfonate) in chemical hood.
2. Extensively rinse the scaffold slices as follows. Transfer slices to a 50 mL conical tube containing 35 mL of 1x PBS; shake by hand or vortex for 30 s; transfer slices to a new 50 mL conical tube containing 35 mL of 1x PBS; shake by hand or vortex for 30 s again.
3. Repeat 10 times or until there are few to no bubbles evident in the rinsate. If many bubbles remain, cease shaking for ~10 s, repeat last step, until there are few to no bubbles.
4. Place the scaffold slices in 2 mL of benzonase buffer (Table of Materials) for set of mouse lungs at room temperature (RT) for 10 min. Then, transfer the slices to 5 mL of benzonase (50 U/mL), rolling at 37 °C for 1 h by a shaker.
NOTE: Warm the benzonase buffer to 37 °C before use.

3. Sterilization and Storage

1. Rinse the scaffold slices with 25 mL of sterilization solution in a 50-mL conical tube placed on a shaker (250 rpm) for 1 h at 37 °C to make them sterile. Repeat this step for a total of two rinses.
2. Store the prepared scaffold slices in sterilization solution at 4 °C.

2. Human Lung Tissue Slice Decellularization Protocol

1. Preparation of slices

1. Visually examine the lung tissue (by eye) to ensure that the tissue is anatomically intact and does not appear to be grossly infected. Grossly disrupted tissues will be torn, ruptured and/or clotted; grossly infected tissues will have pus emanating from the airways and airspaces.
CAUTION! Fresh human tissue is potentially infectious biomaterial and should be handled with standard precautions.
2. Place the lung tissue in a 60-mm sterile Petri dish. Transfer this 60-mm Petri dish to a 100-mm Petri dish. Put these two Petri dishes in the liquid nitrogen container together in order to float the Petri dishes on the surface of the liquid nitrogen and the tissue will be snap frozen to allow precise slicing.
NOTE: The ideal volume of the lung tissue is from (Length 1 cm × Width 1 cm × High 1 cm) to (Length 3.5 cm × Width 3 cm × High 2 cm). Scale up or down as needed for the particular application.
3. Using sterile technique, cut the tissue into 2 mm slices with a multi-knife. Rinse extensively with PBS containing SNP at 1 µg/mL for 1 h.
4. Transfer the slices to a 50-mL tube containing 15 to 25 mL of decellularization solution, maintain at 37 °C, and roll the tube overnight with a shaker at 8 rpm.
5. Extensively rinse the scaffold slices with PBS until there are few to no bubbles left. Place the scaffold slices in the benzonase buffer (10 mL) at RT (20 - 25 °C) for 10 min. Transfer the scaffold slices in a new 50 mL tube containing new benzonase buffer nuclease (15 to 25 mL) with benzonase at 90 U/mL to treat the scaffold slices with for 1 h at 37 °C.
NOTE: Warm the benzonase buffer to 37 °C before use.

2. Sterilization and Storage

1. Rinse the scaffold slices with 25 mL of sterilization solution in a 50-mL conical tube placed on a shaker (250 rpm) for 1 h at 37 °C to make them sterile. Repeat this step once for a total of two rinses. Store the prepared scaffold slices in sterilization solution at 4 °C until use.

3. Preparation of the Scaffold and Seeding of Cells

NOTE: The below protocol is optimized for fibroblast cell lines. Users should determine their own conditions.

1. Immediately prior to culture rinse slices with PBS for 5 min twice. Place slices in a tissue cultured treated, Poly-L-Lysine coated 6-well plate.
NOTE: The slices can roll when removed from PBS. Use forceps to stretch to the corner of the slices to make them even.
2. Incubate at 37 °C for at least 10 min to allow adherence to the bottom of the plate but do NOT dry the slices. Use 3 slices per well. This step is critical.
3. Suspend 10^4 , 10^5 , or 10^6 fibroblasts in 50 μ L of fibroblast medium (**Table of Materials**). Drizzle cells over the slice. Place the seeded slices in the 37 °C incubator with 5% CO₂ for 30 - 60 min. Add 1.85 mL of additional medium to the well and return to the incubator.
NOTE: Before fibroblast seeding in the scaffold, we use regular cell culture flasks to culture the fibroblast. The cells of 80% cell confluence are ready to be used as materials to do scaffold cell culture. Use 0.5 mL 0.25% Trypsin-EDTA to dissociate cells from cell culture flasks, use a hemocytometer to count cells and centrifuge at 188 x g for 5 min, then resuspend in cell culture medium, based on different cell number to add medium by different volume. The final cell concentration will be 10^4 , 10^5 , or 10^6 in 50 μ L.
4. Partially (500 μ L) change medium after 24 h and then every 48 h thereafter for a maximum culture period of 14 days.
NOTE: At this point, scaffolds can be fixed in 4% paraformaldehyde and paraffin embedded for histologic evaluation, stored in TRIzol reagent for RNA isolation, snap frozen for future protein extraction, or used for other purposes as determined by the user.

4. Digestion of the Scaffold

1. Lyophilize decellularized scaffold. Lyse the lyophilized tissue with lysis buffer at 55 °C overnight to obtain the lung ECM solution (about 10 mg dry decellularized human lung will be lysed by 0.5 mL lysis buffer).
2. Centrifuge the lung ECM solution at 3,615 x g for 8 min, collect supernatant, add 0.5 mL of lysis buffer to re-lyse the pellet again at 55 °C overnight.
NOTE: Fibrotic tissue can be difficult to digest and may form chunks of insoluble material.
3. Mix the ECM solution from 4.1 and 4.2, and dialyze to remove the lysis buffer against 4 L of ddH₂O. Repeat three times for a total of four dialysis sessions. Perform the first for at least 1 h, the second overnight, and the third and fourth for at least 1 h.
4. Filter sterilize the purified ECM solution by a 0.45 μ m filter apparatus. Analyze protein concentration of the ECM solution using a protein assay dye reagent concentrate kit (See the **Materials Table**).

5. Stimulation of Cells with ECM Solution

NOTE: This method is optimized for peripheral blood mononuclear cells (PBMCs), users should determine optimal concentration for their specific need.

1. Make the ECM working solution: Mix ECM solution with FBS, penicillin/streptomycin, 5x DMEM and cell culture grade water to make the ECM working solution.
NOTE: Prepare 5x Dulbecco's Modified Eagle Medium (DMEM) by DMEM powder. Dilute 5x DMEM to 1x DMEM in ECM working solution; ECM working solution: 20 μ g/mL ECM protein + 10% FBS + 1% penicillin/streptomycin + 1x DMEM.
2. Use solution of polysucrose and sodium diatrizoate to isolate peripheral blood mononuclear cells (PBMCs) by Ficoll technique^{22,23,24}. Seed 1×10^6 PBMCs in a 12-well-plate. The composition of the cell culture medium is (10% FBS + 1% penicillin/streptomycin + 1x DMEM).
3. Treat PBMCs with ECM solution by adding (50 μ L of ECM working solution + 450 μ L of 1x DMEM) for the final concentration of 1 μ g/mL and 500 μ L of ECM working solution for the final concentration of 10 μ g/mL. The final medium volume is 1 mL per well. Culture for up to 14 days.
CAUTION! Human PBMCs are a potentially infectious biomaterial and should be handled with standard precautions.

Representative Results

The initial steps of this protocol are designed to process intact lung tissue such as that shown in **Figure 1A** to yield an acellular culture substrate such as that shown in **Figure 1B**. This goal requires achieving a balance between complete removal of cellular material and the maintenance of tissue architecture and composition. Thus, evaluation of the scaffold should take these outcomes into account. In terms of decellularization, several approaches can be used to determine the amount of cellular material remaining in the decellularized scaffold. Qualitatively, fluorescence based detection of nuclear material can be performed using 4',6-Diamidino-2-Phenylindole (DAPI) staining followed by fluorescence microscopy. Unlike native tissue, which shows abundant DAPI signal (**Figure 2A**), the decellularized lung will display a complete absence of DAPI staining (**Figure 2A**). Additional evaluation of decellularization can be performed using quantitative DNA fluorescence based assays (**Figure 2B**) which will reveal a nearly complete absence of DNA in the decellularized tissue. Removal of cellular proteins such as beta-actin and major histocompatibility class II (MHCII) can be confirmed by Western blot, where relative to intact lung, the decellularized lung will reveal a complete absence of signal (**Figure 2C**).

When examined histologically, Hematoxylin and Eosin (H&E) or trichrome staining and light microscopy reveals complete absence of cellular material but preserved alveolar architecture (**Figure 3B left**) versus native lung (**Figure 3A left**). Further, evaluation by scanning electron microscopy also reveals an absence of cells but intact alveolar spaces (**Figure 3B right**)¹³. The protocol presented here has not been optimized for studies of the airway or blood vessels, whose tubular structure is quite different from the topography of the parenchyma. It also should be noted here that the decellularization procedure is a delicate balance between removal of cells and preservation of tissue. For example, the high pH and detergent based conditions can degrade tissues leading to a shredded appearing scaffold and an inability to detect intact structural proteins^{25,26}. In contrast, appropriately decellularized tissues will retain collagens and proteoglycans, though glycosaminoglycans may be reduced relative to native tissues (**Figure 4**).

Because cell: matrix interactions are likely to be quite abnormal in the setting of pulmonary fibrosis, we refined this technique for the study of cell: matrix interactions in the context of the diseased lung ECM. Here as shown in **Figure 5A** and **5B**, the slicing technique can be used to decellularize fibrotic tissues removed from experimentally manipulated laboratory animals (**Figure 5A**) or from explanted fibrotic human lungs (**Figure 5B**). Decellularization is achievable (**Figure 5A-5C**) and histologic evaluation reveals the disrupted architecture and ECM accumulation that are the defining features of fibrosis (**Figure 5A-5C**). Mechanical testing at the low deformation range such as would be encountered during normal breathing demonstrates that relative to scaffolds prepared from normal lung tissue, which display tensile properties similar to those reported for intact native lung (**Figure 5D**), scaffolds prepared from fibrotic lungs produce tensile responses that are nearly an order of magnitude greater (**Figure 5D**). When viewed in combination, the above results show that decellularization of mammalian lung slices produces an acellular matrix scaffold retaining many of the gross anatomic, microstructural, biochemical, and biophysical properties of native lung tissue.

Once the scaffolds have been prepared and characterized, they can be used in any number of applications. Many of these involve the transfer of a cell population directly onto the scaffold (**Figure 6**). While the decellularization method was initially developed as the basis for the *ex vivo* generation of functional organs, the procedure described herein is more suitable for mechanistic studies of cellular interactions with the isolated ECM. Thus, the method requires consideration of the cells to be seeded into this system, the culture conditions to be employed, and the readouts to be used to determine responses. For the most part, the quantification can be presented as cells per high powered field or cells per unit lung tissue. Because engraftment can be heterogeneous (**Figure 7**) we have developed a semi-quantitative method to quantify cellular coverage in a two-dimensional system. This objective scoring standard, which is termed the "repopulation index," involves manual determination of cellular content for the entire tissue slice. Since this initial report, we have applied this methodology to study the signaling pathways through which fibroblasts interact with the normal lung cells¹³ (**Figure 8**), as well as to the study of immune cell phenotypes in the setting of scleroderma⁵ (**Figure 9**) both via direct contact with the intact scaffold and with stimulation with the digestible components of the ECM, and macrophage fibroblast crosstalk in the clinical setting of Idiopathic Pulmonary Fibrosis¹⁶ (**Figure 10**).

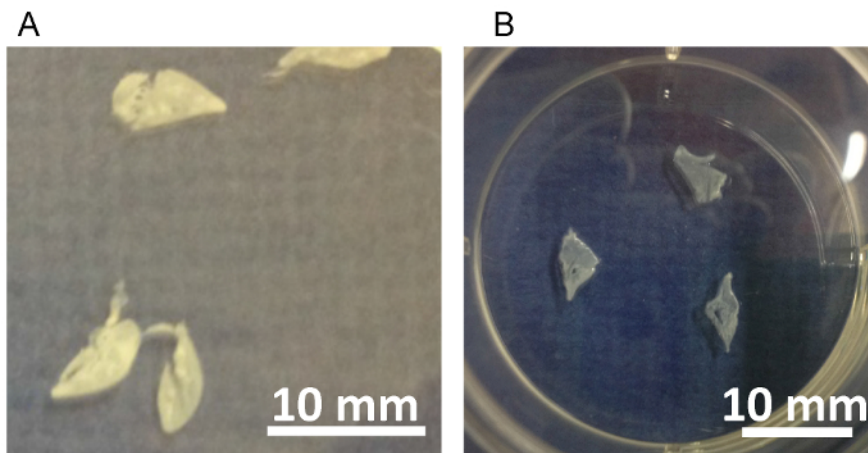


Figure 1: Murine lung scaffolds. Mouse lung slices preceding (A) and immediately following decellularization (B). [Please click here to view a larger version of this figure.](#)

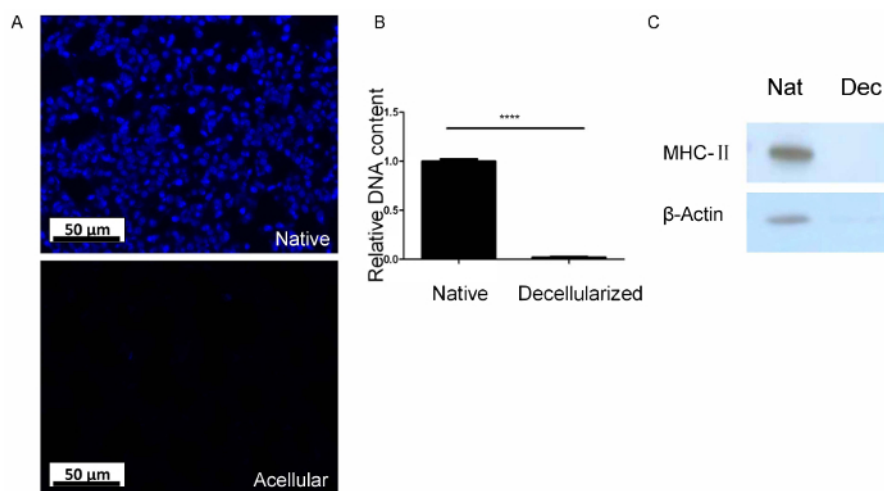


Figure 2: Determination of cellular absence. **A.** DAPI stains confirm presence or absence of genetic material in the ECM. DAPI staining of (top) native mouse lung slices and (bottom) decellularized mouse lung slices. Note the absence of DAPI signal in the bottom panel. **B.** Fluorometric comparison of digested native lung tissue and decellularized lung slices. Error bars show Standard Error of Mean (SEM); **** $p < 0.0005$ by t-test. **C.** Western blot detection of (top) Major histocompatibility complex II (top, MHCII) and beta-actin (β -actin, bottom) in native and decellularized lung slices. Figure reprinted with permission from American Journal of Physiology (AJP)-Lung¹³. [Please click here to view a larger version of this figure.](#)

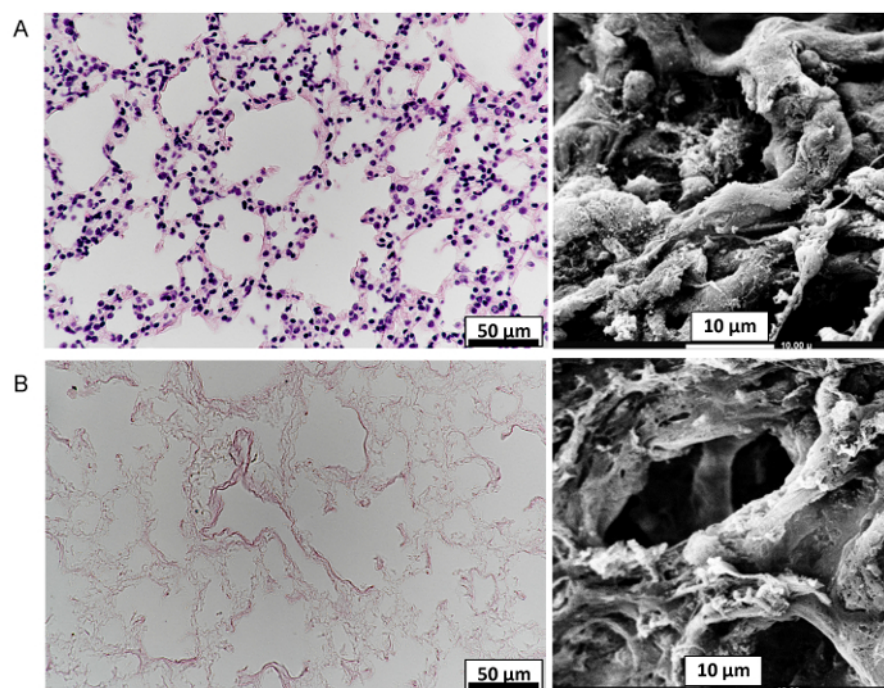


Figure 3: Assessing matrix integrity. **A.** Native mouse lung slices analyzed by H&E staining (left) and scanning electron microscopy (right). **B.** Decellularized mouse lung slices evaluated identically reveal intact alveolar structure and the absence of cells at the microstructural and ultrastructural level. Panels **A** and **B** are reprinted with permission from AJP-Lung¹³. [Please click here to view a larger version of this figure.](#)

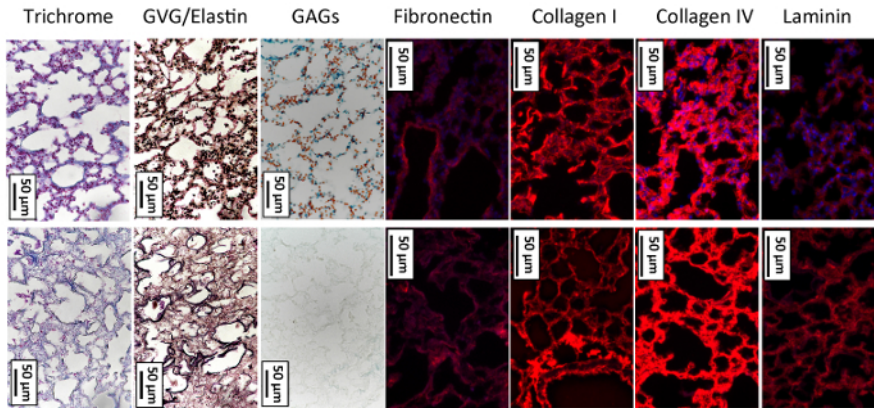


Figure 4: Immunodetection of ECM proteins in native vs. decellularized murine lung slices. Top row shows the appearance of selected ECM proteins in the native lung. Bottom row shows the same proteins detected via immunofluorescence in the decellularized murine lung. Fluorescence images are counterstained with DAPI and panels are reprinted with permission from AJP-Lung¹³. [Please click here to view a larger version of this figure.](#)

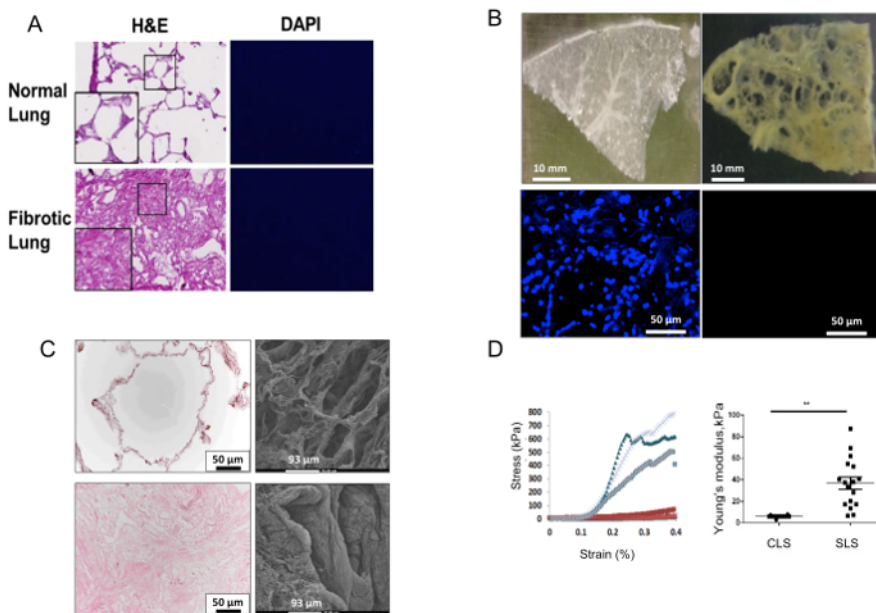


Figure 5: The slice method is amenable for use on fibrotic lungs. **A.** H&E staining (left) and DAPI staining (right) on decellularized mouse lung slices prepared from (top) normal mouse lungs and (bottom) the lungs of mice in which fibrosis had been generated by the intratracheal instillation of bleomycin. **B.** Top: Gross appearance of decellularized lung slices prepared from (left) control lung and (right) fibrotic human lung (in this case, Scleroderma lung). Bottom: DAPI staining of native and decellularized SSc-ILD lung. **C.** Comparison of H&E staining (left) and scanning electron microscopy (right) of a control lung scaffold (CLS, top) and fibrotic lung (in this case scleroderma, SLS, bottom) reveals disrupted tissue architecture and ECM accumulation in the fibrotic scaffolds. **D.** Tensile testing performed via Instron 5848 reveals that relative to scaffolds prepared from control lung tissue (red), scaffolds prepared from explanted scleroderma lungs demonstrate excessive stiffness as measured by Young's modulus. Panel **(A)** reprinted with permission from JBC¹⁷. Panels **(B-D)** reprinted with permission from Arthritis and Rheumatology⁵. Error bars show SEM; **p < 0.01 by t-test. [Please click here to view a larger version of this figure.](#)

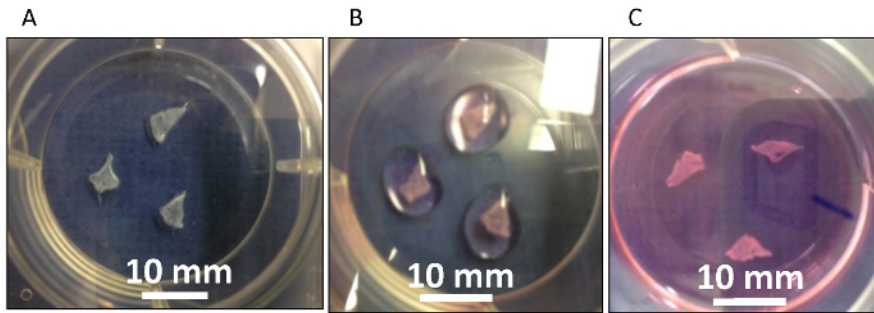


Figure 6: Seeding of cells. **A.** Scaffolds are allowed to adhere to the bottom of the culture well for 10 min. **B.** Cells suspended in a small amount of medium are drizzled over the scaffolds and placed in the incubator for 30 - 60 min. **C.** Additional media is added to the well. Figure is reprinted with permission from AJP-Lung¹³. [Please click here to view a larger version of this figure.](#)

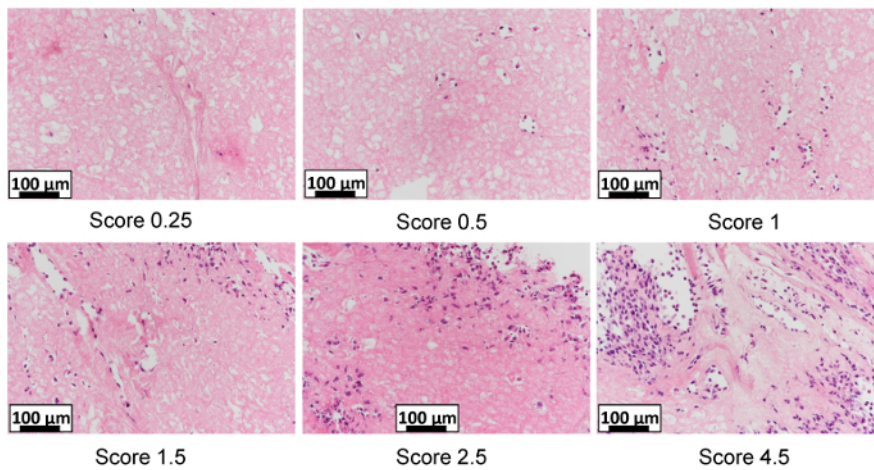


Figure 7: Scoring the cellular coverage of the scaffold. Cellular coverage of the scaffold can range from nearly absent to nearly complete. This image presents a semiquantitative scoring system developed by our group to assist with interpretation of engraftment efficiency. [Please click here to view a larger version of this figure.](#)

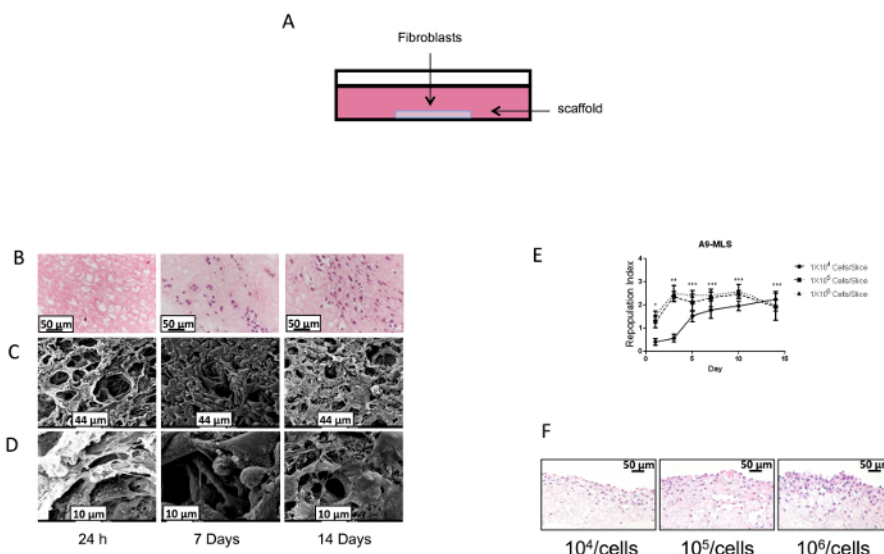


Figure 8: Analysis of engraftment. **A.** Schematic of experiment in which fibroblasts are inoculated directly into the scaffold. **B-D.** Fibroblast seeded mouse lung scaffolds examined in the transverse plane show altered cell density following seeding of cells. A time dependent increases in cellular coverage in the two-dimensional axis can be seen by H&E staining (**B**), low power scanning electron microscopy (SEM) (**C**), and high-power SEM (**D**). **E.** Varying the initial concentration of cells alters engraftment at early and intermediate but not later timepoints. Error bars show SEM. **F.** Examination of the scaffolds in the sagittal plane demonstrates in addition to two-dimensional coverage, seeded cells display the ability to invade into the scaffold for three-dimensional engraftment as well. Figure is reprinted with permission from AJP-Lung¹³. [Please click here to view a larger version of this figure.](#)

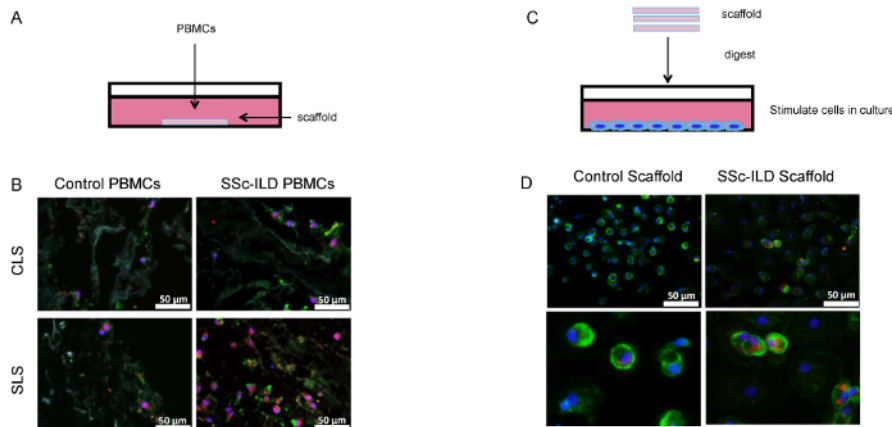


Figure 9: Immune cell phenotypes in the setting of scleroderma. **A.** Schematic of experiment in which peripheral blood mononuclear cells (PBMCs) can be seeded directly onto the scaffolds to evaluate the interaction of circulating immune cells with the decellularized lung ECM. **B.** Representative immunofluorescence of control and SSs-ILD PBMCs (**B**) seeded into control lung scaffolds (CLS) and Scleroderma lung scaffold (SLS). Cells are stained for CD45 (green), Pro-Collagen Iα1 (red) and counterstained with DAPI (blue). **C.** Schematic demonstrating that scaffolds can also be digested to generate an ECM containing solution that can be used to stimulate cultured cells. **D.** Representative immunostaining of PBMCs obtained from a control donor grown in the presence of digested control lung scaffolds (CLS) or SLS. As above, cells are stained for CD45 (green), Pro-Collagen Iα1 (red) and counterstained with DAPI (blue). Scale bars, 50 μm. Images reprinted with permission from Arthritis and Rheumatology⁵. [Please click here to view a larger version of this figure.](#)

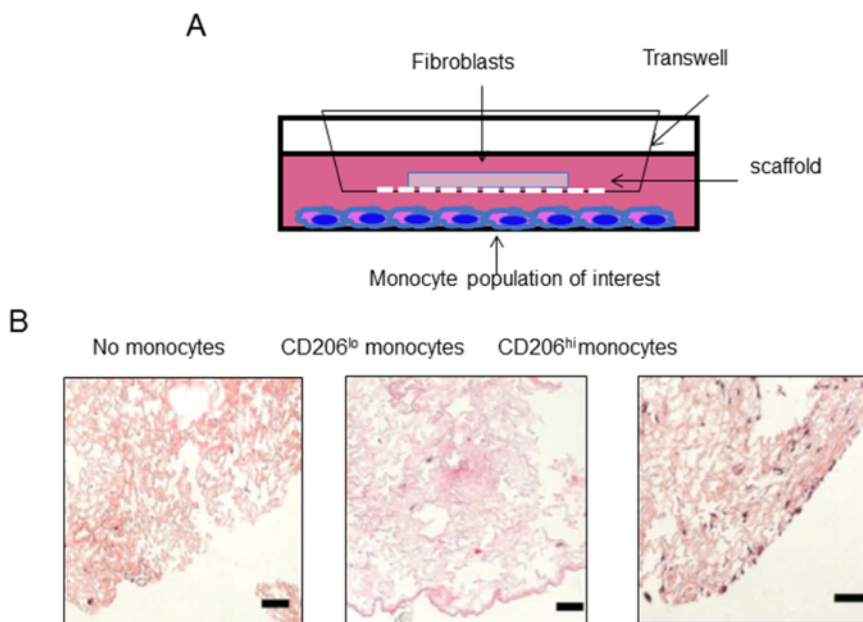


Figure 10: Monocyte/Macrophage fibroblast crosstalk in the clinical setting of Idiopathic Pulmonary Fibrosis. **A.** Schematic demonstrating that scaffolds can also be used to study cellular crosstalk in the mammalian lung. Here, human lung scaffolds are placed on a Transwell insert and seeded with cells of interest (in this case human fibroblasts). A second population is placed on the bottom of the plate (in this case human monocytes selected based on their expression of the scavenger receptor CD206). The effect of this intervention on fibroblast engraftment is ascertained. **B.** Low power images of fibroblast seeded human lung scaffolds grown in the presence of (left to right) no primary monocytes, CD206^{lo} primary human monocytes, and CD206^{hi} primary human monocytes obtained from patients with IPF. Scale bars, 200 μm. Images reprinted with permission from Science Translational Medicine¹⁶. [Please click here to view a larger version of this figure.](#)

Discussion

The application of bioengineering based strategies to studies of tissue remodeling and fibrosis has the potential to greatly advance the understanding of cellular responses to the normal and diseased extracellular matrix. The method reported herein represents several potential advances over the use of classical cell culture strategies. For example, the plastic and glass culture plates used for the studies of mesenchymal cell biology possess a stiffness exceeding that of fibrotic tissue by several orders of magnitude, which introduces a nonphysiologic tensile property into the modeling system. Plastic and glass are also artificially bioinert and typically require coating with purified ECM, which does not entirely recapitulate the complexity of the ECM present in the intact lung. Furthermore, these modeling systems are also largely two dimensional

and lack the topographic cues that cells would encounter in an intact organ. However, in order to ensure optimal performance of the model, attention to the following aspects is required.

One extremely important part of this protocol is the rinsing steps that occur following overnight rolling decellularization. Retention of the alkaline detergent will harshen the conditions such that tissue architecture is no longer intact. The protein components of the ECM may be compromised as well. Because the decellularization solution is detergent based, it forms bubbles during the rinsing steps. Once the bubbles are no longer visible during rinsing, the solution is likely removed. However, we generally recommend rinsing at least once more in order to be fully certain that no residual solution is retained.

Another critical part of this protocol is the sterilization step. Because primary tissues are derived from living organisms that are colonized with commensurate organisms, all of the starting material used in this protocol should be considered contaminated and in need of sterilization. This requirement is especially true of the human lungs. Grossly infected appearing lung tissue should not be used in this protocol as it will be nearly impossible to achieve adequate sterilization even with the stringent steps outlined herein. Similarly, if at any step during the processing or culturing evidence of bacterial or fungal contamination is observed (usually visible colonies floating on the surface of the culture medium), samples should be discarded and the protocol re-initiated.

Another important aspect is the stabilization of the decellularized scaffold during the culture process. We have found that unanchored matrices rise to the surface of the culture medium. This complication results in the curling and contraction of the scaffold into a rounded structure which impedes cell growth while simultaneously creating an uninterpretable tissue mass. While it is generally quite easy to extend the decellularized slice derived from nonfibrotic lung, extension and adherence of the fibrotic lung may require the formation of footlike processes to exert traction on the culture plate. During this adhesion step it is imperative that the scaffold not dry out. If the decellularized matrices appear prone to desiccation, addition of a small amount of sterile PBS may be employed to maintain adequate moisture prior to cell seeding.

One limitation of the procedure is the uneven engraftment that is sometimes observed. This heterogeneity might result from regional differences in ECM composition or structure that are native to the intact tissue or are induced during the decellularization process. It is not clear whether engraftment and expansion of seeded cells are due to initial differences in adherence, survival, or proliferation of the seeded cells. Another issue is that the seeding of a single cell population might not accurately reflect how cells respond when native and inflammatory cell populations are present. In fact, our work in this area demonstrates that seeded cells behave differently depending on the concomitant presence of structural cells such as lung epithelia and inflammatory cells such as macrophages. The model also omits important aspects of lung physiology such as inspiratory/expiratory cycle, blood flow, gas exchange, and the presence of epithelial lining fluid containing surfactant and other bioactive molecules. Nevertheless, the methods reported herein hold great potential to advance the study of cell: matrix interactions in a variety of translational settings and experimental contexts.

Disclosures

The authors have no disclosures relevant to this manuscript.

Acknowledgements

This study was supported by grants from the Scleroderma Foundation (H.S.) and the N.I.H (R01HL109233, R01HL125850, both to E.L.H.).

References

1. Rosenberg, H.F., Masterson J.C., Furuta, G.T. Eosinophils, probiotics, and the microbiome. *Journal of Leukocyte Biology*. **10** (5), 881 (2016).
2. Duan, M., Hibbs, M.L., Chen, W. The contributions of lung macrophage and monocyte heterogeneity to influenza pathogenesis. *Immunology and Cell Biology*. **95** (3), 225 (2017).
3. Fujita, Y., Kosaka, N., Araya, J., Kuwano, K., Ochiya, T., Extracellular vesicles in lung microenvironment and pathogenesis. *Trends in Molecular Medicine*. (9), 533 (2015).
4. Petersen, T. H. *et al.* Tissue-engineered lungs for in vivo implantation. *Science*. **329**, 538-541 (2010).
5. Sun, H. *et al.* Netrin-1 regulates fibrocyte accumulation in the decellularized fibrotic sclerodermatous lung microenvironment and in bleomycin-induced pulmonary fibrosis. *Arthritis & Rheumatism*. **68**, 1251-1261 (2016).
6. Hynes R.O., Naba, A. Overview of the Matrisome-An Inventory of Extracellular Matrix Constituents and Functions. *Cold Spring Harbor Perspectives Biology*. (4), 1 (2012).
7. Wynn, T. A. Integrating mechanisms of pulmonary fibrosis. *Journal of Experimental Medicine*. (7), 1339 (2011).
8. Geiser, T. Idiopathic pulmonary fibrosis-a disorder of alveolar wound repair? *Swiss Medical Weekly*. (29-30), 405 (2003).
9. Selman, M., King, T.E., Pardo, A. Idiopathic pulmonary fibrosis: prevailing and evolving hypotheses about its pathogenesis and implications for therapy. *Ann Intern Med*. (2), 136 (2001).
10. Moore, M. W., & Herzog, E. L. Regulation and relevance of myofibroblast responses in idiopathic pulmonary fibrosis. *Current Pathobiology Reports*. **1**, 199-208 (2013).
11. Nelson, C. M., & Bissell, M. J. Of extracellular matrix, scaffolds, and signaling: Tissue architecture regulates development, homeostasis, and cancer. *Annual Review Of Cell & Developmental Biology*. **22**, 287-309 (2006).
12. Song, J. J., & Ott, H. C. Organ engineering based on decellularized matrix scaffolds. *Trends in Molecular Medicine*. **17**, 424-432 (2011).
13. Sun, H. *et al.* Fibroblast engraftment in the decellularized mouse lung occurs via a β 1-integrin-dependent, fak-dependent pathway that is mediated by erk and opposed by akt. *American Journal of Physiology-Lung Cell and Molecular Physiology*. **306**, L463-L475 (2014).
14. Calle, E.A. *et al.* Fate of distal lung epithelium cultured in a decellularized lung extracellular matrix. *Tissue Engineering Part A*. **21**, 1916-1928 (2015).
15. Parker, M. W. *et al.* Fibrotic extracellular matrix activates a profibrotic positive feedback loop. *The Journal of Clinical Investigation*. **124**, 1622-1635 (2014).

16. Zhou, Y. *et al.* Chitinase 3-like 1 suppresses injury and promotes fibroproliferative responses in mammalian lung fibrosis. *Science Translational Medicine*. **6**, 240ra276-240ra276 (2014).
17. Southern, B. D., Tschumperlin, D. J. *et al.* Matrix-driven myosin ii mediates the pro-fibrotic fibroblast phenotype. *Journal of Biological Chemistry*. **291**, 6083-6095 (2016).
18. Field, K. J., White, W. J., Lang, C. M. Anaesthetic effects of chloral hydrate, pentobarbitone and urethane in adult male rats. *Lab Animals*. **27**, 258-269 (1993).
19. Lancelin, W., & Guerrero Plata, A. Isolation of Mouse Lung Dendritic cells. *Journal of Visualized Experiments*. **57**, 3563 (2011).
20. Han, H., & Ziegler, S. F. Bronchoalveolar Lavage and Lung Tissue Digestion. *Bio-protocol*. **3** (16), e859 (2013).
21. Calle, E. A., Petersen, T. H., Niklason, L. E. Procedure for lung engineering. *Journal of Visualized Experiments*. 2651-2651 (2011).
22. Amos, D.B., and Pool, P. HLA typing. *Manual of Clinical Immunology*. **797** (1976).
23. Winchester, R.J., Ross, G. Methods for enumerating lymphocyte populations. *Manual of Clinical Immunology*. **64** (1976).
24. Thorsby, E., Bratlie, A. A rapid method for preparation of pure lymphocyte suspensions. *Histocompatibility Testing*. **665** (1970).
25. Calle, E.A. *et al.* Targeted proteomics effectively quantifies differences between native lung and detergent-decellularized lung extracellular matrices. *Acta Biomaterialia*. **46**, 91 (2016).
26. Wallis, J.M. *et al.* Comparative Assessment of Detergent-Based Protocols for Mouse Lung De-Cellularization and Re-Cellularization. *Tissue Engineering Part C*. **6**, 420 (2012).